# Optimizing the Performance of Open-Type Refrigerated Display Cabinets: Block Schemes and Key Tasks

Tadas Vengalis[*]

Department of Mechanical and Materials Engineering, Vilnius Gediminas Technical University, 10105 Vilnius, Lithuania

[*] Correspondence: Tadas Vengalis (tadas.vengalis@vilniustech.lt)

**Abstract:** The performance of open-type refrigerated display cabinets has been rigorously examined through the development and application of two comprehensive block schemes, which integrate numerical simulations with experimental research. Central to these schemes is the use of a simplified two-dimensional, time-dependent computational fluid dynamics (CFD) model, designed to evaluate and optimize airflow patterns, thermal behavior, and energy efficiency within the cabinets. The numerical simulations, validated against experimental data, demonstrate that the strategic design and configuration of air curtains and internal components significantly mitigate the impact of ambient air, thereby reducing temperature fluctuations that are critical for maintaining food quality and safety. The application of these block schemes has been shown to enhance energy efficiency and reduce electrical consumption, contributing to operational cost savings. The strong correlation between CFD results and experimental findings underscores the reliability of these models for accurately representing real-world conditions. Future investigations could benefit from exploring additional geometric configurations and incorporating more advanced CFD techniques to further refine the performance of refrigerated display systems. This integrated approach offers a robust framework for improving the operational effectiveness and food preservation capabilities of open-type refrigerated display cabinets.

**Keywords:** Open-type refrigerated display cabinet; Air curtain; Air velocity; Computational fluid dynamics simulations; Honeycomb; Heat transfer; Temperature

## 1 Introduction

Industrial refrigeration equipment plays a crucial role in retail stores and the food supply chain [1]. Maintaining temperature control in these systems is essential for preserving food quality and safety, with specific storage temperatures detailed in the EN ISO 23953-2:2015 [2] standard. Retail refrigerators are categorized into open and closed types. Open refrigeration cabinets, commonly used for perishable products, provide easy access for customers [3], but they are less energy-efficient and fail to maintain the required temperature consistently. Air infiltration in open cabinets can account for 67-77% of all heat exchange with the environment [4].

In contrast, closed refrigeration cabinets are more energy-efficient and better at maintaining stable temperatures [5]. Research indicates that open cabinets consume about 79% more electrical energy than closed ones, making closed-type equipment up to 1.3 times more efficient [5]. Heat flows in industrial refrigerators are described by the Navier-Stokes and Reynolds equations, which require various numerical schemes and algorithms to solve. Numerical models, whether two-dimensional or three-dimensional, are essential for accurately simulating airflow and temperature dynamics. While three-dimensional models are more accurate, they demand substantial computational resources. Turbulent flow simulations in industrial refrigeration typically use methods like Large Eddy Simulation (LES), Reynolds-Averaged Navier-Stokes (RANS), and Menter's Shear-Stress Transport (SST) models, with the RANS k-epsilon ($k - \varepsilon$) model being popular for its computational efficiency [6–8].

Open-type refrigerated display cabinets are vital in retail food stores for proper food storage and trading, as they attract buyers and increase sales [3]. These cabinets usually store food at temperatures between -1 and +7℃ (3M2 temperature category), which is suitable for dairy products, sandwiches, green salad, and cooked meat instead of minced or raw meat, which require temperatures between -1 and +4℃ (3M0 temperature category) (EN ISO

23953-2:2015 [2]). Open cabinets allow free access to food due to the absence of physical barriers, but this design leads to significant air penetration and increased heat load, resulting in higher energy consumption [4]. Replacing open cabinets with doored ones can improve food quality, save energy, and reduce temperature fluctuations [5]. Despite their advantages, open cabinets are often preferred by customers due to their easier access [9].

Numerical simulations can enhance cabinet designs by improving air curtain performance and predicting thermal behavior economically [10]. For example, three-dimensional CFD simulations of open-top display units using the porous-jump model have demonstrated the benefits of modifications like air-guiding strips, which enhance air curtain efficiency and reduce cooling capacity requirements [11].

Open-type multi-deck semi-vertical refrigerated display cabinets are popular in retail for their ability to attract customers and increase sales without physical barriers. Cabinets with two air curtains are more energy-efficient than those with a single one, forming a stronger barrier between ambient and inside air [8]. Numerous studies have focused on improving these cabinets' efficiency through numerical and experimental investigations, optimizing air curtain performance to reduce energy consumption and enhance temperature stability [3, 4].

Researchers have used CFD models to simulate airflow and temperature distribution in these cabinets, comparing numerical results with experimental data. Optimization strategies, such as the support vector machine (SVM) algorithm, significantly reduce cooling loss and energy consumption [12]. The ambient environment's impact on cabinet performance has also been studied, showing that different placement methods can influence efficiency. For instance, placing cabinets back-to-back rather than face-to-face can improve refrigeration performance and lower food temperatures [13]. Customer interactions also affect the cold chain, with studies indicating that customer movement increases air temperature and thermal load [14].

This study outlines a methodology utilizing block schemes and key tasks to investigate the performance of open-type refrigerated display cabinets. It synthesizes data from previous CFD and experimental research studies [15–18], summarizing key tasks and illustrating the results using block schemes. The aim is to demonstrate the use of numerical simulations in a commercial refrigerated unit manufacturing company as a faster and more efficient method for improving performance, reducing the reliance solely on experimental research.

## 2 Materials and Methods

### 2.1 Description of the Open-Type Refrigerated Display Cabinets
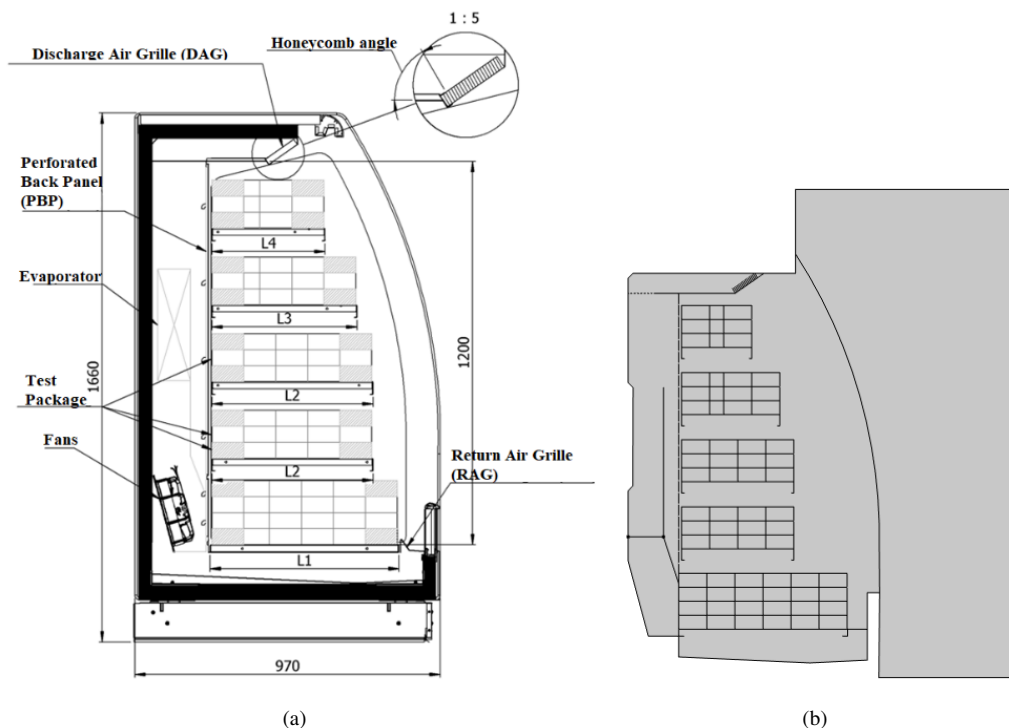


**Figure 1.** Two-dimensional side view of (a) The Ordc-1 refrigerated cabinet and (b) The corresponding geometric model [18]

In this study, two geometric models of industrial refrigerators with distinct height and width characteristics were analyzed. These models are simplified versions, created by removing non-essential internal and external components

that do not impact the refrigerator's functionality. The dimensions of the experimental models (height × depth) are Ordc-1 (1660 × 970) and Ordc-2 (2005 × 845), while the simplified geometric models are Ordc-1 (1745 × 1400) and Ordc-2 (2500 × 2280). These models were designed to include part of the surrounding environment necessary for forming the air curtain and its effect on the environment. A two-dimensional cross-section of the Ordc-1 refrigerator is shown in subgraph (a) of Figure 1, while the corresponding simplified two-dimensional computational geometric model is shown in subgraph (b) of Figure 1. In the geometric model of Ordc-1, 66 M-packages (100 × 50 mm) and 9 M-packages (50 × 50 mm) were utilized, with 20 of the 100 × 50 mm packages equipped with virtual temperature sensors. The comparison of the two sides reveals that the calculated model excludes parts of the walls, roof, and bottom. Sheet elements are depicted by lines, with the bending radius of the sheet metal replaced by square connections. In the numerical modeling performed using COMSOL Multiphysics 5.4, the sheets were assigned material properties and given thickness.

The temperature inside the Ordc-1 display case is regulated by two separate cooling airflows. The initial airflow descends from the top of the display case, creating an air curtain, while the second flow moves from the back of the case toward the front, where the two flows combine. The combined airflow is pulled back into the display case through suction grilles, where it is redirected by four fans through the evaporator, ensuring a continuous flow of cooled air throughout the system.
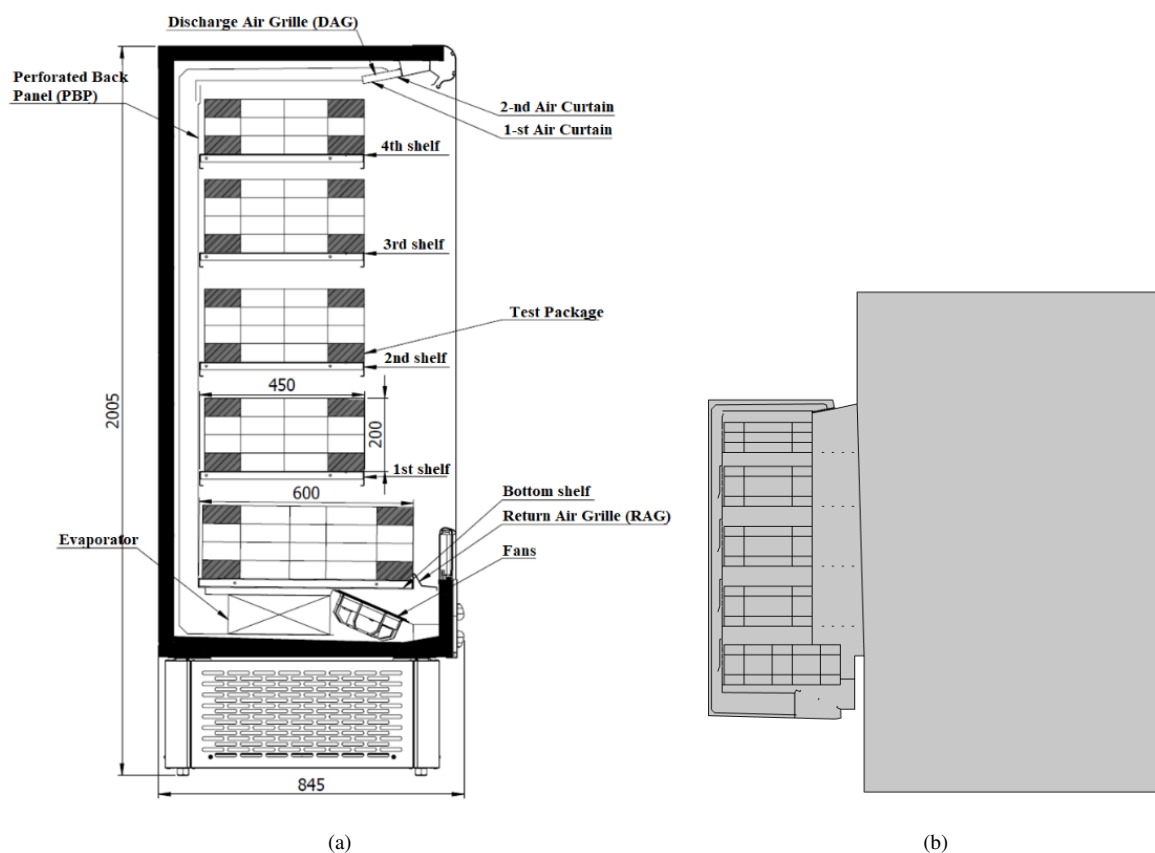


**Figure 2.** Two-dimensional side view of (a) The Ordc-2 refrigerated cabinet and (b) The corresponding geometric model [17]

The Ordc-2 model differs from the first model in terms of size, geometry, and arrangement of the fans. The industrial refrigerator has the ability to create one or two air curtains. The two-layer air curtains are designed for taller refrigerated display cases. This model has a number of unique features compared to standard single air curtain display cases. The cooled air is pushed upwards by the fans in the internal air curtain. The internal air curtain is created when cooled air is distributed through the rear wall and directed over the display case. The second air curtain is produced by moving the intake air through a separate path. This air is directed over the display case through an enclosed channel. A mix of 80% of the internal air curtain temperature and 20% of the external air curtain temperature is used to calculate the temperature inside a refrigerated display case. The Ordc-2 geometric model has 84 M-packages with virtual temperature sensors. A two-dimensional cross-section of the Ordc-2 refrigerator is shown in subgraph (a) of Figure 2, while the corresponding simplified two-dimensional computational geometric

model is shown in subgraph (b) of Figure 2.

## 2.2 Mathematical Model and Boundary Conditions

The equation describing heat transfer in fluids within the problem domain $\Omega$ is given as follows [19, 20]:

$$\rho C_p \left( \frac{\partial T}{\partial t} + u \cdot \nabla T \right) + \nabla \cdot (q + q_r) = \alpha_p T \left( \frac{\partial p}{\partial t} + u \cdot \nabla p \right) + \tau : \nabla u + Q \tag{1}$$

When fluids or gases are in motion, they move in all spatial directions, but their flow can often be simplified and described in two-dimensional space. This assumption is useful as it reduces the complexity of the problem by decreasing the number of variables involved. This two-dimensional flow retains all the essential properties needed to describe the processes through mathematical equations, and extending these equations to three-dimensional forms is a direct process. The key equations that govern fluid motion are as follows:

a) Continuity equation (two-dimensional space-Cartesian plane):

$$\frac{\partial u}{\partial x} + \frac{\partial v}{\partial y} = 0 \tag{2}$$

b) Momentum equation, also known as the Navier-Stokes equation, which describes the conservation of momentum within a fluid.

$$\rho \left( \frac{D\vec{V}}{Dt} \right) = \nabla P + \mu \nabla^2 \vec{V} \tag{3}$$

c) Temperature transport (energy) equation, which governs temperature distribution in two-dimensional space, as derived by Schlichting [21] and discussed by Vaitiekūnas [22].

$$\left( \frac{\partial T}{\partial t} + u \frac{\partial T}{\partial x} + v \frac{\partial T}{\partial y} \right) = \frac{\lambda}{\rho c_p} \left( \frac{\partial^2 T}{\partial x^2} + \frac{\partial^2 T}{\partial y^2} \right) + \frac{\lambda}{\rho c_p} \left[ 2 \left( \frac{\partial u}{\partial x} \right)^2 + 2 \left( \frac{\partial v}{\partial y} \right)^2 + \left( \frac{\partial u}{\partial x} + \frac{\partial v}{\partial y} \right) \right] \tag{4}$$

The $k - \varepsilon$ model was used for turbulence simulation. It is one of seven turbulence models available in the COMSOL Multiphysics software package. This model is based on the RANS approach, where the Navier-Stokes equations are averaged over time to produce a set of differential equations for the averaged variables, such as velocity and pressure. This set of equations differs from the original Navier-Stokes equations only by the inclusion of the Reynolds stress tensor. This tensor is expressed using Boussinesq's hypothesis, which relates it to the gradients of the averaged velocities:

$$-\rho \overline{u_l' u_j'} = \mu_t \left[ \frac{\partial u_i}{\partial x_j} + \frac{\partial u_j}{\partial x_i} \right] - \frac{2}{3} \left[ \rho k + \mu_t \frac{\partial u_k}{\partial x_k} \right] \delta_{ij} \tag{5}$$

The values of $k$ and $\varepsilon$ were determined from the respective transport equations:

$$\frac{\partial(\rho k)}{\partial t} + \nabla \cdot (\rho k \vec{u}) = \nabla \cdot \left( \left( \mu + \frac{\mu_t}{\sigma_k} \right) \nabla k \right) + G_k + G_b - \rho \varepsilon - Y_m + S_k \tag{6}$$

$$\frac{\partial(\rho \varepsilon)}{\partial t} + \nabla \cdot (\rho \varepsilon \vec{u}) = \nabla \cdot \left( \left( \mu + \frac{\mu_t}{\sigma_\varepsilon} \right) \nabla \varepsilon \right) + C_{1\varepsilon} \frac{\varepsilon}{k} (G_k + C_{3\varepsilon} G_b) - C_{2\varepsilon} \frac{\varepsilon^2}{k} + S_\varepsilon \tag{7}$$

The efficiency of the air curtain is described by the formula for the air penetration coefficient ($\eta$) as follows:

$$\eta = \left| \frac{T_{DAG} - T_{RAG}}{T_{DAG} - T_{AM}} \right| \tag{8}$$

To streamline the numerical modeling while preserving the key characteristics of the process within the problem domain $\Omega$ (Figure 3), the following assumptions were made:

- The process is in a steady state, meaning the air temperature remains constant over time.
- Mass transfer from the load to the air (mass loss) is excluded.
- Moisture transfer processes are not included.
- The effects of the evaporator and fan are represented by the incoming air stream.
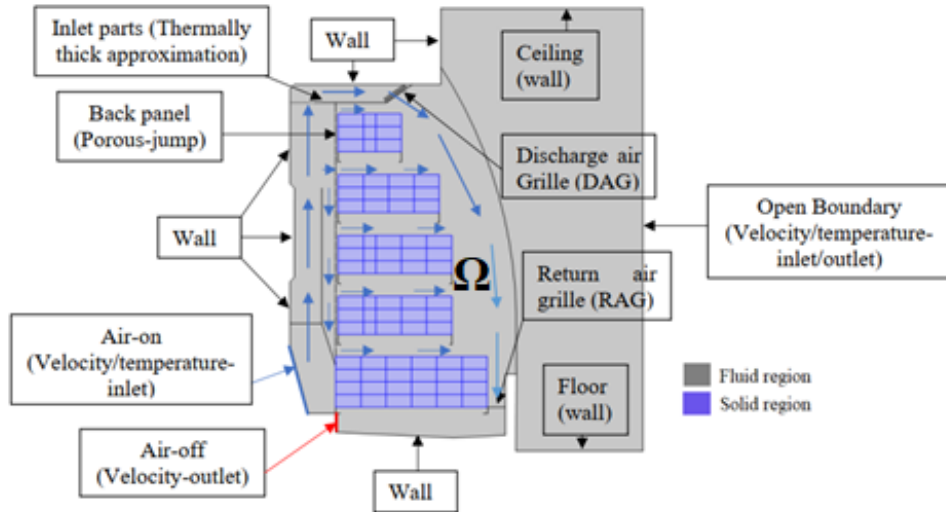
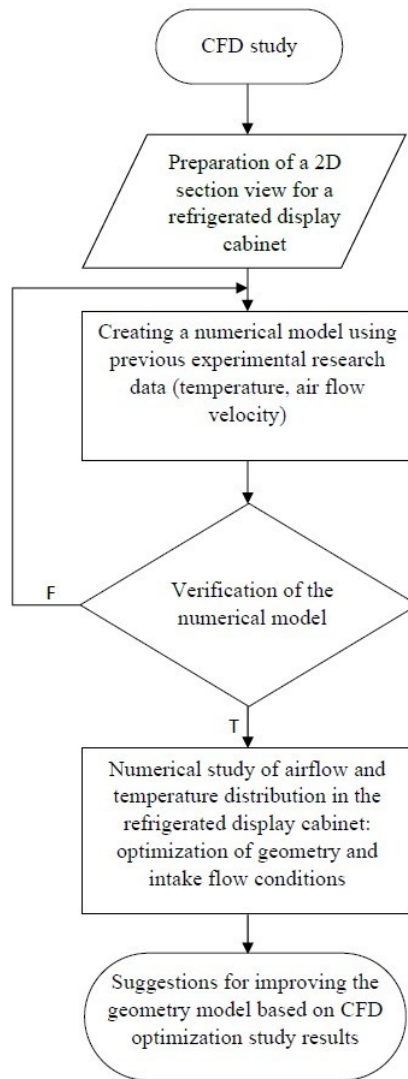**Figure 3.** Zones and boundary conditions of an open-type refrigerator model [18]



**Figure 4.** Initial block scheme of numerical research

## 2.3 Block Schemes for Numerical and Experimental Research

Block schemes are commonly used to investigate refrigerated display cabinets. For this purpose, two block schemes were developed. Figure 4 presents a scheme for studying newly designed industrial refrigeration units. This study uses results from previous experimental research to establish initial conditions. Efficiency improvements identified through the numerical study were then applied to refine the industrial refrigeration unit.

Figure 5 presents an algorithm scheme applied to an already manufactured industrial refrigerator, which can be implemented in two ways. In the first method, after conducting experimental studies, the input data and results are transferred to a numerical model. This approach creates an accurate numerical model based on experimental data, which is used to improve the existing geometry. However, it is time-consuming because the industrial refrigerator must be removed from the laboratory after the experimental study and returned once the numerical study results are obtained to continue the research. Alternatively, in the second method, numerical and experimental studies are carried out concurrently for quicker results. The numerical model is prepared before the experimental study, and during the study, it is validated while examining flow efficiency. This approach achieves optimal results in the least amount of time when addressing flow problems.
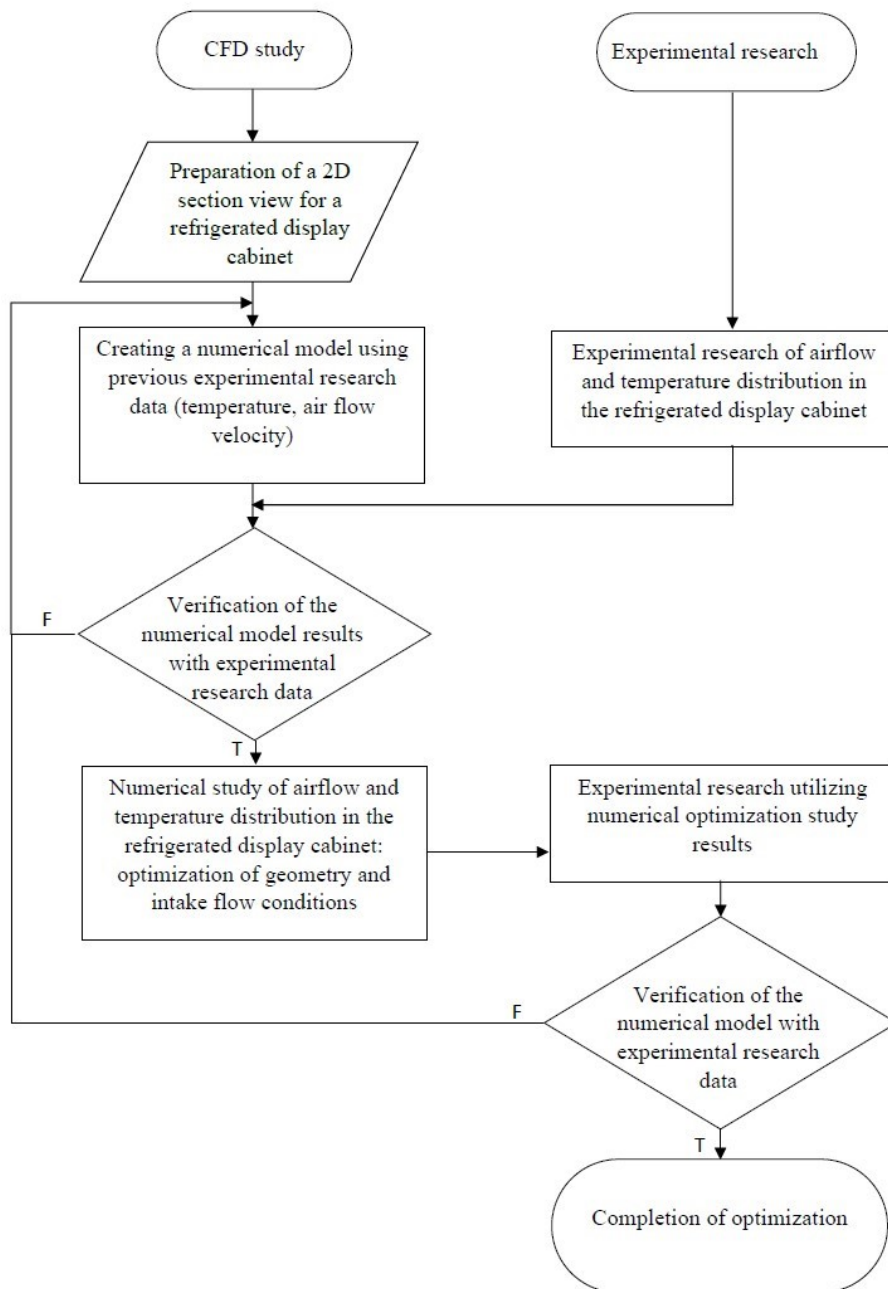
Figure 5. Block scheme of numerical and experimental research

## 2.4 Tasks of Numerical and Experimental Research

Based on the block schemes, the following tasks were proposed for the numerical and experimental studies. For the numerical CFD studies, as shown in Figure 4, the primary tasks are to assess how the inclination angle of the honeycomb affects the air curtain's performance and analyze the temperature distribution within the test package.

For numerical and experimental studies, as outlined in Figure 5, three key tasks need to be addressed, namely, combined temperature in the test package, combined velocity of thermal flows, and temperature distribution in the test package.

To evaluate the full performance of the refrigerated cabinet in the testing chamber, the temperature of thermal flows, the temperature distribution in the test package, and the electrical energy consumption were measured for experimental research.

These tasks are crucial in clarifying the main parameters influencing the performance of refrigerated displays. Depending on the specific case of refrigerated cabinets, these tasks may need to be adjusted to achieve better performance results. Details of the numerical procedures, boundary conditions, and experimental research methods have been described by Vengalis and Moksin [15–18].

## 3 Results and Discussion

## 3.1 CFD Research Results of the Ordc-1 Refrigerated Display Cabinet



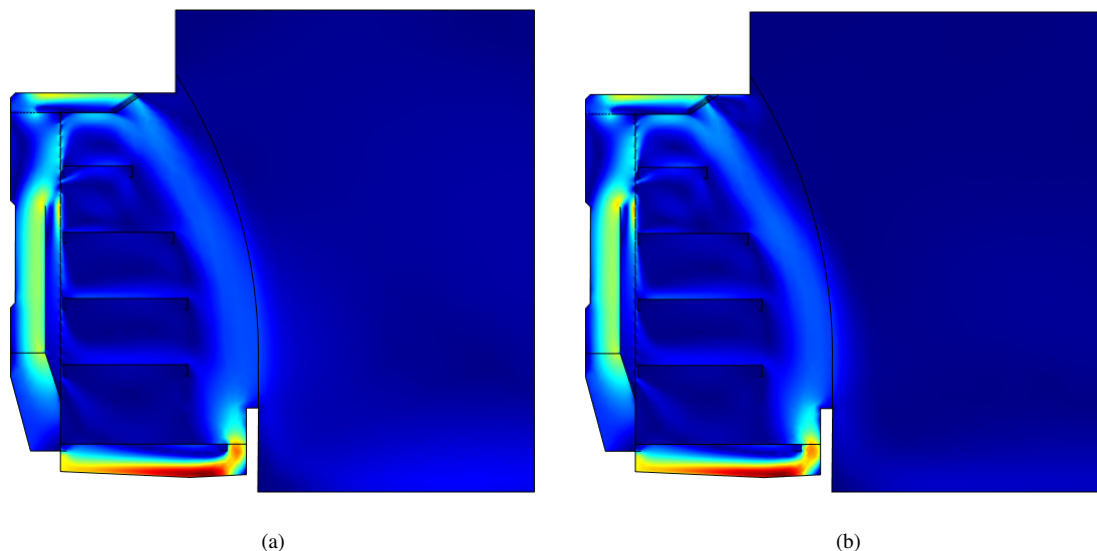(a)                                                    (b)

**Figure 6.** Airflow velocity distribution inside the empty refrigerated cabinet obtained for different honeycomb angles (a) 45°; (b) 55° [18]

According to the key tasks of the CFD studies, the first task is to check the inclination angle of the honeycomb for the performance of the refrigerated display cabinet. Figure 6 shows two different angles of the Ordc-1 display cabinet. This figure also presents the profiles of a fully formed airflow curtain in the middle plane of the empty refrigerated cabinet. More details about this research can be found in previous work [15, 18].

The standard angle before the optimization process was 45°, and the 55° angle was chosen after simulations. A 5° step was used in the study to investigate the influence of the inclination angle. Figure 7 shows the relationship between intake air temperature and honeycomb angle for an empty refrigerated cabinet. It indicates that the intake air temperature is lowest at a 55° angle, suggesting that this angle is optimal for an empty cabinet.

Figure 8 presents a graph of intake air temperature versus honeycomb angle for a fully loaded refrigerated cabinet. It shows higher intake airflow temperatures compared to an empty refrigerated cabinet. The reduction in the inside volume of the refrigerated cabinet due to the test packages increases the velocity of airflows. This increased velocity impacts the internal airflows and the airflow curtain, extending the heat exchange duration between the airflow curtain and the environment, which in turn affects the intake temperature. By combining the results from Figure 7 and Figure 8, a honeycomb angle of 55° was selected for subsequent tasks as it demonstrated the best performance for the refrigerated cabinet.

Following the efficiency studies of the single air curtain, the average temperatures of the M-packages in both optimized and non-optimized industrial refrigerators were calculated, as illustrated in Figure 9. In this figure, M-packages positioned near the rear perforated wall are labeled with the letter B followed by numbers, while those near

the front are labeled with the letter F followed by numbers. The packages are numbered from 1 to 10, from top to bottom. The temperatures were determined using a 24-hour thermal flow analysis.
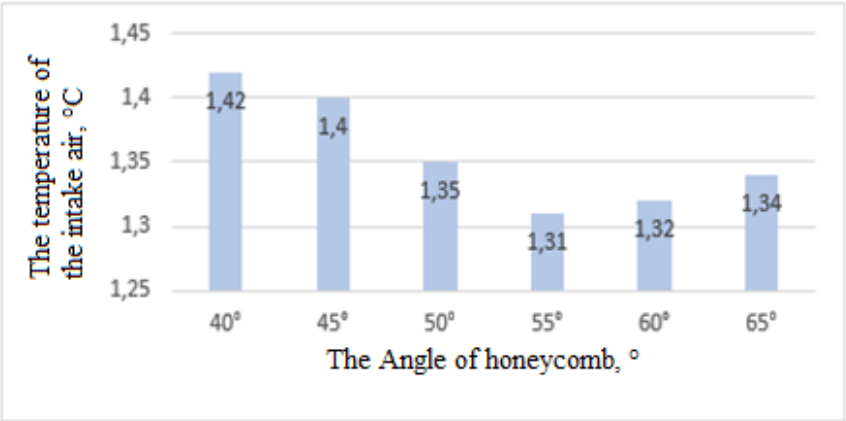


**Figure 7.** Airflow temperature at the intake grill versus honeycomb inclination angle (empty cabinet) [15]
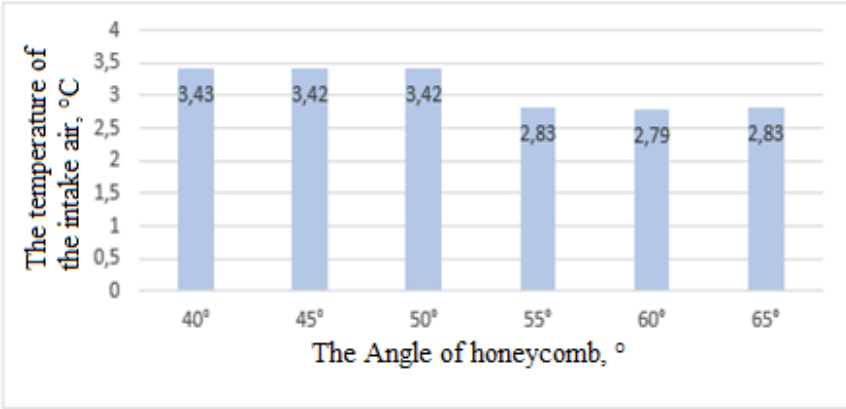


**Figure 8.** Airflow temperature at the intake grill versus honeycomb inclination angle (full cabinet) [15]
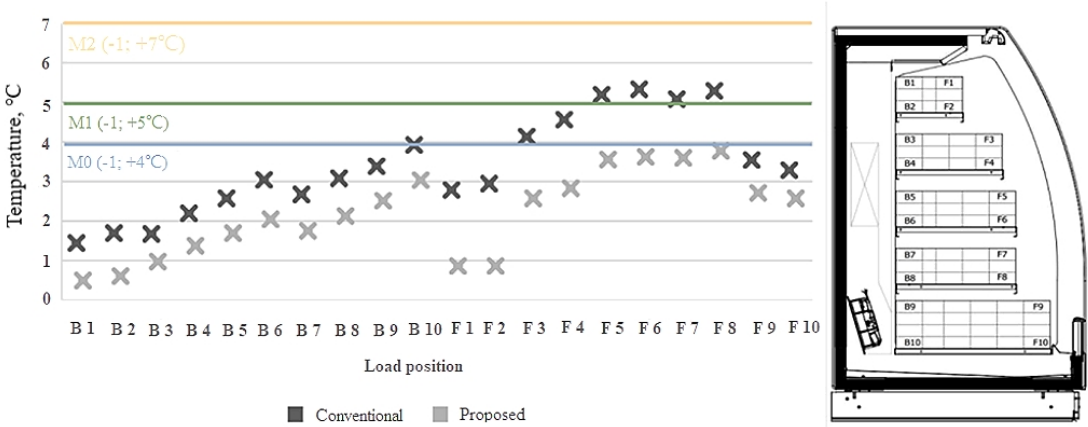


**Figure 9.** Temperature distribution of M-packages in the middle plane of the Ordc-1 refrigerated cabinet [18]

In the unmodified refrigerator, the lowest recorded temperature is +1.4°C at position B1, while the highest is +5.4°C at position F6. The average temperature across all M-packages is +3.38°C. In the modified refrigerator, the lowest temperature is +0.5°C, also at position B1, and the highest is +3.8°C at position F8. The average temperature of the M-packages in this version is +2.18°C. These results indicate that the enhanced air curtain provides better

protection for the front M-packages, with the highest temperature now occurring one shelf lower compared to the unmodified refrigerator. This suggests increased warm air infiltration at the top shelf.

Additionally, Figure 9 illustrates more significant temperature variations at positions F1 and F2, which result from the expanded airflow of the curtain directed towards the M-packages. The unmodified refrigerator is appropriate for storing food products in the 3M2 temperature class (ranging from -1°C to +7°C), whereas the modified version is suitable for the 3M0 temperature class (ranging from -1°C to +4°C).

The calculated results of CFD studies may differ from experimental results due to the intake conditions chosen in previous experimental works. However, accurate calculation results can be achieved by using the block scheme presented in Figure 5.

### 3.2 CFD Studies and Experimental Research Results of the Ordc-2 Refrigerated Display Cabinet

According to the block scheme in Figure 5, the main task is to combine numerical and experimental results. Figure 10 compares the average temperature of the shelves obtained experimentally with those from numerical simulations. In the experimental study, the average temperature of the food products on different shelves is 0.1-0.3°C higher than that obtained in the simulation, and the average temperature of all M-packages is 0.2°C higher. This comparison indicates that the numerical model is suitable not only for studying a single airflow curtain but also for analyzing two airflow curtains with an error margin of 0.1-0.3°C.
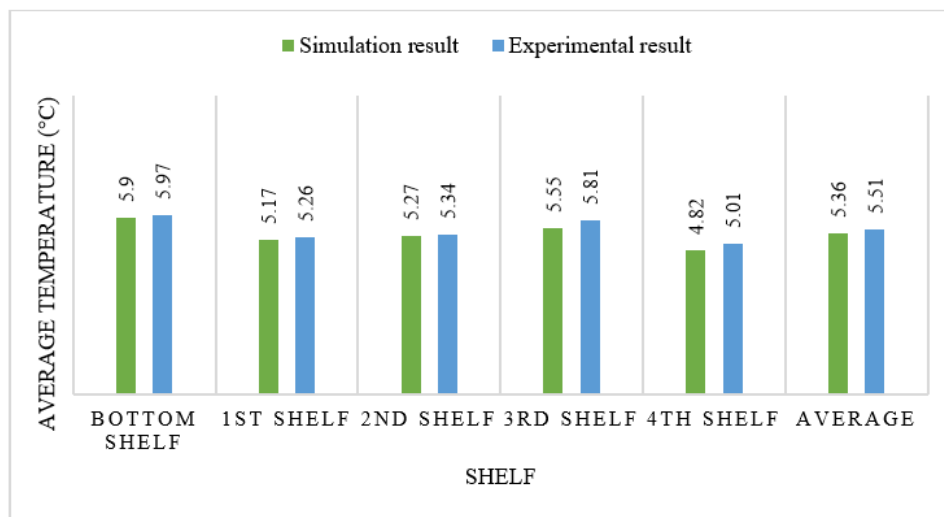


**Figure 10.** Comparison of the food temperatures obtained by CFD and experimentally [16]
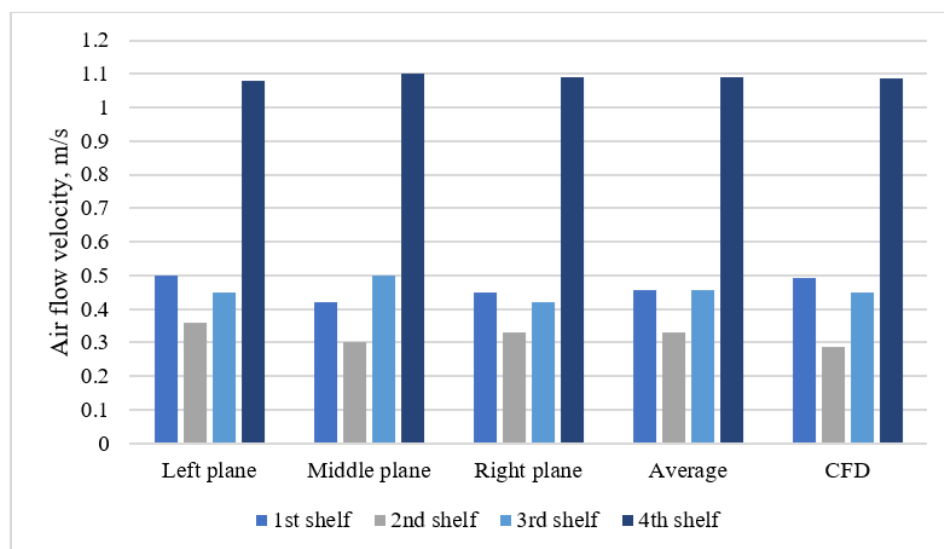


**Figure 11.** Comparison of airflow velocities in Ordc-2 with a double air curtain: CFD results versus experimental data [16]
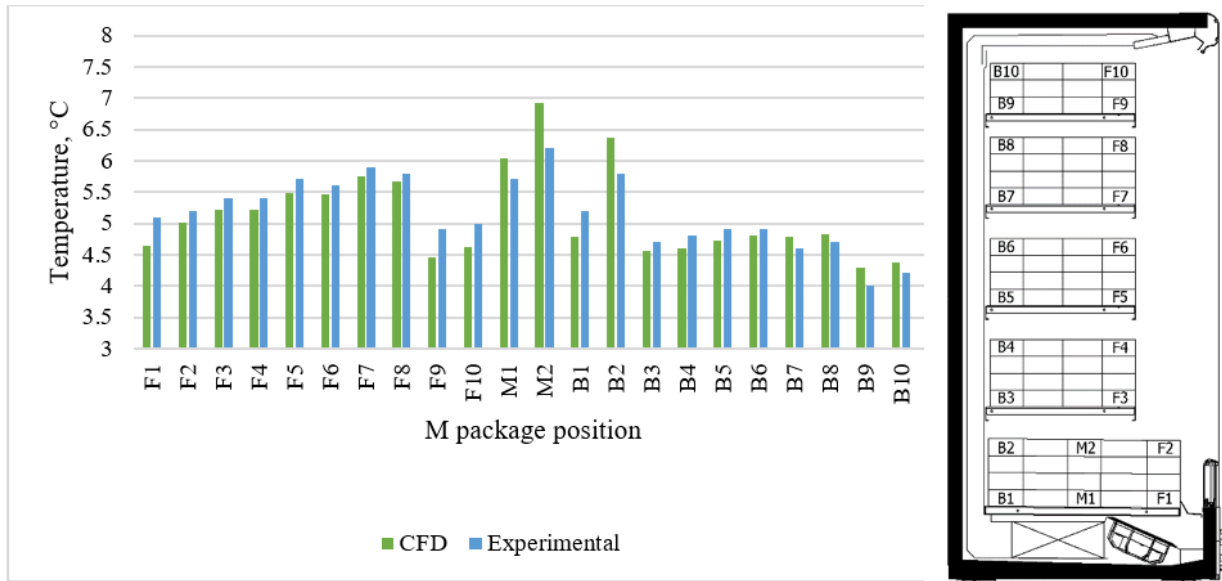
**Figure 12.** Temperature distribution of food products in the middle plane of the Ordc-2 refrigerated cabinet (CFD simulation and experimental research data)

Figure 11 presents a comparison between the airflow velocities obtained through modeling and those measured experimentally. For the experimental measurements, a Testo 405-V1 hot wire anemometer was used, which has a measurement tolerance of ±0.1 m/s and is capable of measuring airflows ranging from 0 to 2 m/s. The comparison reveals that the dispersion of results is within ±0.1 m/s, aligning with the anemometer's tolerance. The smallest error is observed on the fourth shelf, which is closest to the honeycomb structure. Conversely, as the measurements move downward, the spread of results increases, with the largest discrepancies occurring at the first shelf.

After validating the numerical model, it is essential to combine the performance results of the refrigerated display cabinet. Figure 12 shows the temperature distribution of a refrigerated display cabinet with two layers of airflow curtains within the test package. The average temperature of the M-package in the CFD study was calculated to be 5.12°C, while the experimental study measured it at 5.17°C. These results demonstrate the accuracy of the CFD model when combined with experimental data. More details about this research can be found in previous work [16].

This study demonstrates that using the block scheme (Figure 5) for CFD and experimental research can enhance the accuracy of CFD models when combined with experimental data. The improved accuracy of the CFD model can be utilized in future performance research.

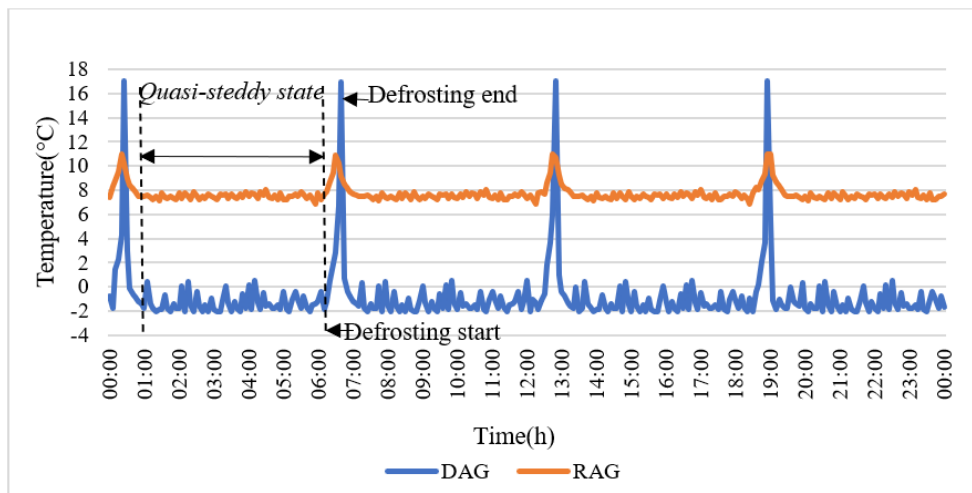### 3.3 Experimental Research Results



**Figure 13.** Air temperature measured in DAG and RAG as a function of time (unmodified cabinet, average of measurements in three planes) [17]

Full experimental research following CFD performance studies is crucial for investigating the entire refrigeration cycle. While numerical studies are calculated under steady-state conditions, experimental research covers all stages of the refrigeration process. Figure 13 shows the temperatures of airflow in the Discharge Air Grille (DAG) and Return Air Grille (RAG) of the unmodified Ordc-1 refrigerated display cabinet. The 24-hour graph illustrates four cycles of refrigeration, each consisting of a quasi-steady state and a defrosting process. During defrosting, the airflow temperature rises to 20°C, potentially negatively impacting the M-package temperature. More details about this research can be found in previous work [17].

In the quasi-steady state, the average air temperature in the DAG is -1.36°C, and it is +7.50°C in the RAG. The air temperature in the DAG varies between -1.90 and 0.50°C, while it ranges from +7.00 to +8.00°C in the RAG (Figure 13).

The temperature versus time graph for the modified Ordc-1 refrigerated cabinet is presented in Figure 14. The average air temperature measured in the DAG in the quasi-steady state is -0.58°C, while the temperature in the RAG is +6.52°C. During the quasi-steady state, the DAG temperature ranges from -1.7 to +0.5°C, and the RAG temperature ranges from +5.90 to +6.90°C.
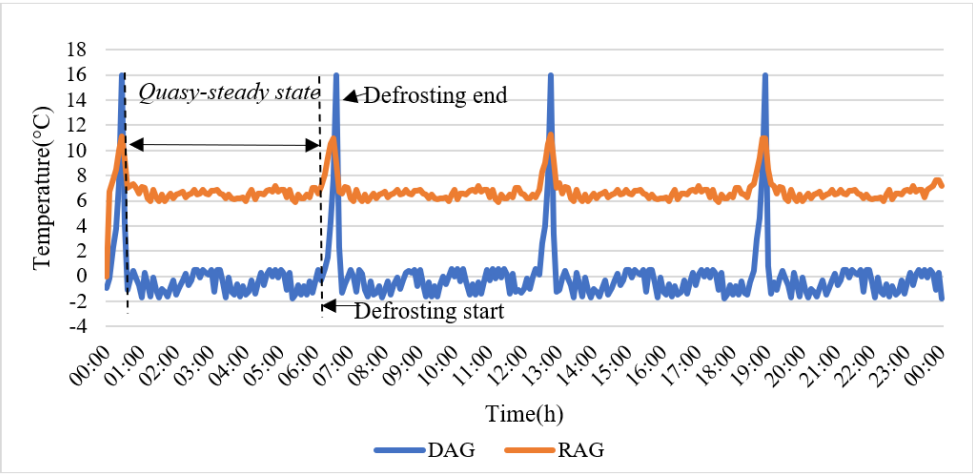


**Figure 14.** Air temperature measured in DAG and RAG as a function of time (modified cabinet, average of measurements in three planes) [17]
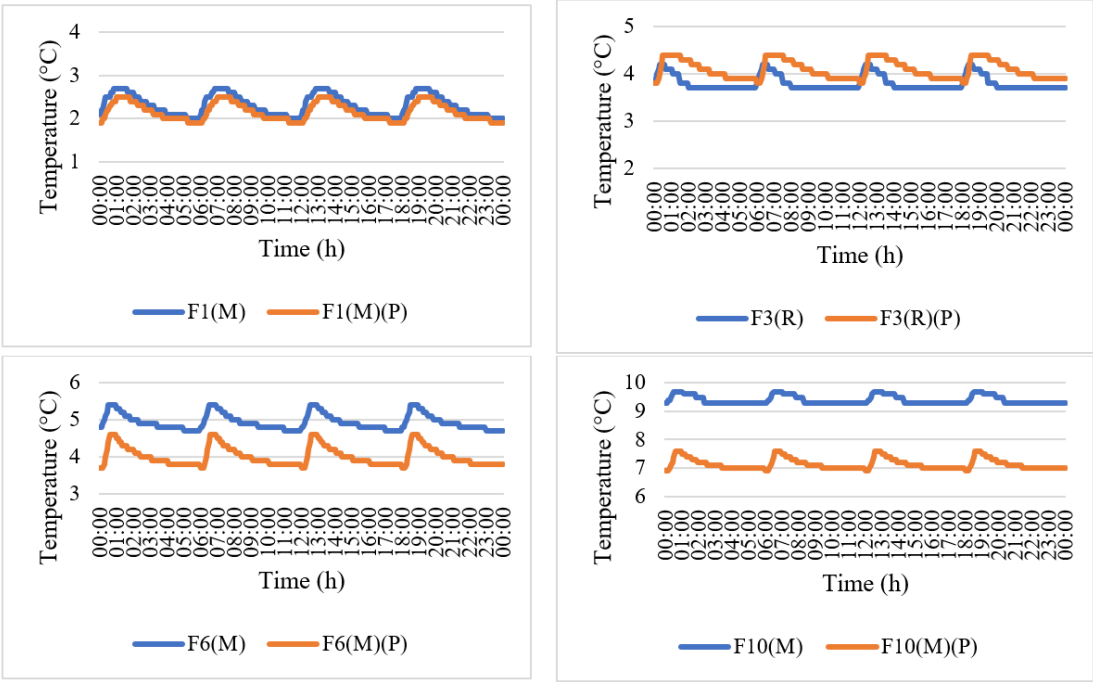


**Figure 15.** Distribution of the temperatures of the M-packages [17]

144

Figure 13 and Figure 14 are typically used to compare the performance of the proposed model against the standard model. Analyzing these graphs helps in understanding the benefits of the upgrade. In this case, the intake airflow temperature in the modified refrigerated cabinet is up to 1°C lower than in the unmodified version. This temperature difference indicates that the modified version has a more effective airflow curtain, which better protects the internal volume from environmental influences.

Temperature measurement of the M-package over 24 hours is crucial for indicating temperature changes at various positions of the M-package. Four graphs in Figure 15 show the temperature of the M-package at the F1, F3, F6, and F10 locations (M-middle plane, R-right plane, L-left plane, P- modified refrigerated cabinet). These measurements help in understanding the temperature distribution and performance of the refrigerated cabinet.

The graphs in Figure 15 depict temperature changes over 24 hours at various marked positions within the refrigerated cabinet. The comparison between the standard and modified refrigerated cabinets demonstrates their performance, revealing that most positions in the modified cabinet show a temperature drop. Notably, the graph for the F3(R) position indicates that the M-package experiences higher temperatures in the modified cabinet compared to the standard version. This can be attributed to the improved airflow and more uniform temperature distribution throughout the modified refrigerated cabinet.

The electrical consumption graphs in Figure 16 and Figure 17 illustrate the energy usage over a 24-hour work cycle. The unmodified version of the refrigerated cabinet consumed 24.91 kWh, whereas the modified version consumed 19.22 kWh over the same period [17]. Analyzing these graphs allows for the assessment of the refrigerated cabinet's performance based on power consumption. The reduced energy usage and lower temperatures in the modified cabinet highlight the effectiveness of the optimization.
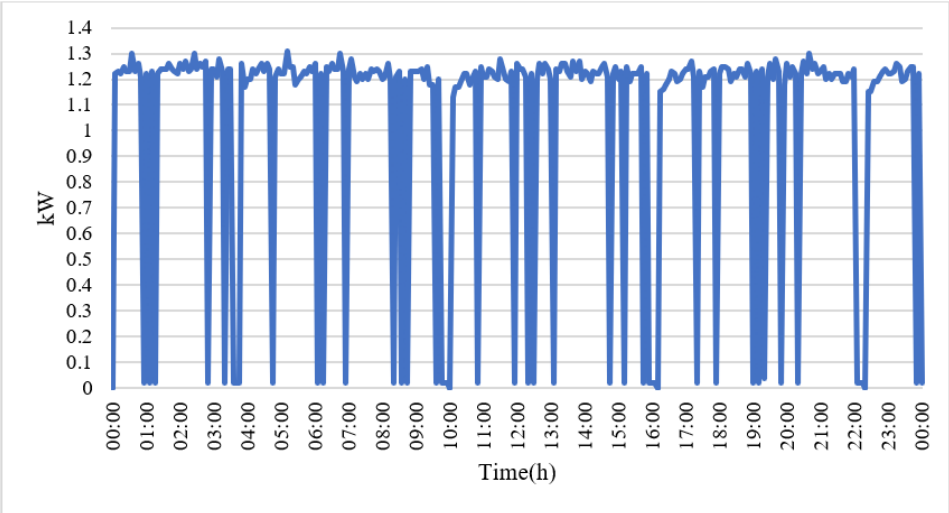


**Figure 16.** The 24-hour electrical energy consumption graph of the unmodified refrigerated cabinet [17]
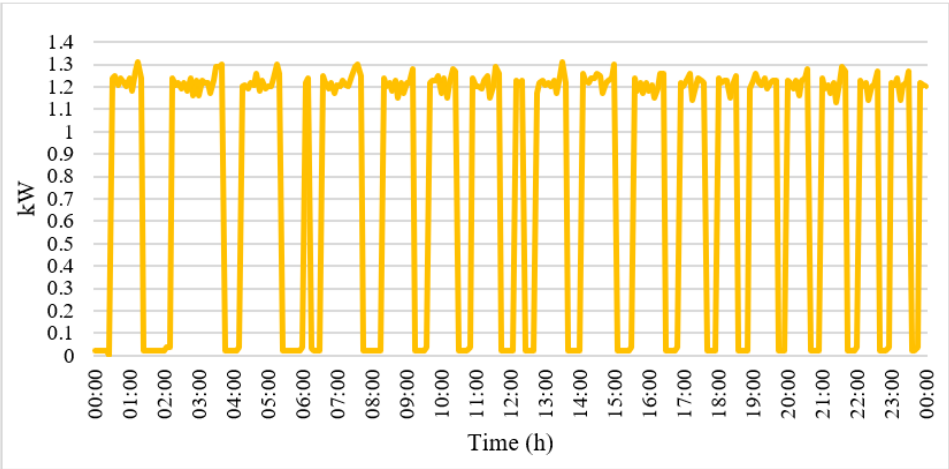


**Figure 17.** The 24-hour electrical energy consumption graph of the modified refrigerated cabinet [17]

## 4 Conclusions and Recommendations

The block schemes and tasks for CFD and experimental research outlined in this study illustrate the optimization process for both open and closed types of refrigerated display cabinets. These block schemes identify essential tasks and demonstrate the benefits of optimization through the described key tasks and results. Implementing this methodology in the manufacturing of refrigerated cabinets can reduce laboratory work time, as two-dimensional CFD modeling often yields superior results compared to relying solely on experimental investigations.

Future research on the performance of refrigerated display cabinets should focus on developing accurate two-dimensional models for components such as the back panel, honeycomb, and intake grille to further enhance their performance.

### Data Availability

The data used to support the findings of this study are available from the corresponding author upon request.

### Conflicts of Interest

The authors declare that they have no conflicts of interest.

### References

[1] N. Chaomuang, O. Laguerre, and D. Flick, "Experimental analysis of heat transfer and airflow in a closed refrigerated display cabinet," *J. Food Eng.*, vol. 224, pp. 101–114, 2019. https://doi.org/10.1016/j.jfoodeng.2018.09.009

[2] International Organization for Standardization, "Refrigerated display cabinets—Part 2: Classification, requirements and test conditions," 2023. https://www.iso.org/obp/ui/en/#iso:std:iso:23953:-2:ed-3:v1:en

[3] Y. G. Chen and X. L. Yuan, "Experimental study of the performance of single-band air curtains for a multi-deck refrigerated display cabinet," *J. Food Eng.*, vol. 69, pp. 261–267, 2005. https://doi.org/10.1016/j.jfoodeng.2004.08.016

[4] B. A. Fricke and B. R. Becker, "Doored display cases: They save energy, don't lose sales," *Ashrae J.*, vol. 52, no. 9, pp. 18–26, 2010.

[5] B. Fricke and B. Becker, "Energy use of doored and open vertical refrigerated display cases," in *International Refrigeration and Air Conditioning Conference*, Indianapolis, 2010.

[6] F. A. Alzuwaid, Y. T. Ge, S. A. Tassou, and J. Sun, "The novel use of phase change materials in an open type refrigerated display cabinet: A theoretical investigation," *Appl. Energy*, vol. 180, pp. 76–85, 2016. https://doi.org/10.1016/j.apenergy.2016.07.088

[7] N. Chaomuang, O. Laguerre, and D. Flick, "A simplified heat transfer model of a closed refrigerated display cabinet," *Therm. Sci. Eng. Prog.*, vol. 17, p. 100494, 2020. https://doi.org/10.1016/j.tsep.2020.100494

[8] A. M. Foster, M. Madge, and J. A. Evans, "The use of CFD to improve the performance of a chilled multi-deck retail display cabinet," *Int. J. Refrig.*, vol. 28, pp. 698–705, 2004. https://doi.org/10.1016/j.ijrefrig.2004.12.009

[9] J. Sun, K. M. Tsamos, and S. A. Tassou, "CFD comparisons of open-type refrigerated display cabinets with/without air guiding strips," *Enrgy. Proced.*, vol. 123, pp. 54–61, 2017. https://doi.org/10.1016/j.egypro.2017.07.284

[10] A. Rai, J. Sun, and S. A. Tassou, "Numerical investigation of the protective mechanisms of air curtain in a refrigerated truck during door openings," *Enrgy. Proced.*, vol. 161, pp. 216–223, 2019. https://doi.org/10.1016/j.egypro.2019.02.084

[11] K. M. Tsamos, H. Mroue, J. Sun, S. A. Tassou, N. Nicholls, and G. Smith, "Energy savings potential in using cold-shelves innovation for multi-deck open front refrigerated cabinets," *Enrgy. Proced.*, vol. 161, pp. 292–299, 2019. https://doi.org/10.1016/j.egypro.2019.02.094

[12] Z. Cao, H. Han, and B. Gu, "A novel optimization strategy for the design of air curtains for open vertical refrigerated display cases," *Appl. Therm. Eng.*, vol. 31, pp. 3098–3105, 2011. https://doi.org/10.1016/j.applthermaleng.2010.10.025

[13] P. Yuan, Q. Zeng, Z. Lei, Y. Wu, and C. Hu, "Experimental and numerical study of heat transfer and fluid flow characteristics with different placement of multi-deck display cabinet in supermarket," *Open Phys.*, vol. 19, no. 1, pp. 256–265, 2021. https://doi.org/10.1515/phys-2021-0023

[14] S. M. Nascimento, G. G. Heidinger, P. D. Gaspar, and P. D. Silva, "Numerical and experimental evaluation of the aerodynamic drag of the air curtain in vertical open refrigerated display cases," in *25th IIR International Congress of Refrigeration (ICR 2019)*, Monreal, Canada, 2019, pp. 3437–3444. https://doi.org/10.18462/iir.icr.2019.0861

[15] T. Vengalis and V. Mokšin, "CFD simulation of heat transfer and airflows in an open refrigerated display cabinet," *IOP Conf. Ser.: Mater. Sci. Eng.*, vol. 1239, p. 012005, 2022. https://doi.org/10.1088/1757-899X/1239/1/012005

[16] T. Vengalis and V. Mokšin, "Experimental and numerical study of the performance of an open-type multi-deck refrigerated cabinet with single and dual air curtain," *Appl. Sci.*, vol. 13, no. 16, p. 9080, 2023. https://doi.org/10.3390/app13169080

[17] T. Vengalis and V. Mokšin, "Experimental study of the performance of open-type refrigerated display cabinet," *J. Eng. Proc. Manage.*, vol. 15, no. 1, pp. 24–30, 2023. https://doi.org/10.61458/jepm2301024V

[18] T. Vengalis and V. Mokšin, "2D CFD simulation of dynamic heat transfer in an open type refrigerated display cabinet," *Appl. Sci.*, vol. 12, no. 14, p. 6916, 2022. https://doi.org/10.3390/app12146916

[19] R. B. Bird, W. E. Stewart, and E. N. Lightfoot, *Transport Phenomena*, 2nd ed.   John Wiley & Sons, 2002.

[20] Comsol, "Heat transfer module: User's guide," 2018. https://doc.comsol.com/5.4/doc/com.comsol.help.heat/HeatTransferModuleUsersGuide.pdf

[21] H. Schlichting, *Boundary-Layer Theory*.   New York: McGraw-Hill, 1979.

[22] P. Vaitiekūnas, *Šilumos Mainų Matematinis Modeliavimas*.   Vilnius: Technika, 2007.